

**An Investigation into the  
Feasibility of Measuring  
Flow-Induced Pressures on  
the Surface of a Model in the  
AMRL Water Tunnel**

Lincoln P. Erm

DSTO-TN-0323

**DISTRIBUTION STATEMENT A**  
Approved for Public Release  
Distribution Unlimited

20010430 048

# An Investigation into the Feasibility of Measuring Flow-Induced Pressures on the Surface of a Model in the AMRL Water Tunnel

*Lincoln P. Erm*

**Air Operations Division  
Aeronautical and Maritime Research Laboratory**

DSTO-TN-0323

## **ABSTRACT**

A study has been undertaken to assess the feasibility of measuring flow-induced pressures on the surface of a model in the AMRL flow-visualization water tunnel. These pressures are extremely small due to the low free-stream velocities generally used for flow-visualization experiments in the tunnel. For a free-stream velocity of 0.1 m/s, flow-induced pressures are typically less than about 15 Pa. In the past the pressures could not be measured accurately since suitable pressure transducers were not available. In this report it is shown that it is now possible to measure the pressures using a modern highly-sensitive transducer. Flow-induced pressures were measured on a delta wing in the AMRL water tunnel, and at the same time the vortical flow over the wing was visualized, enabling the loading on the wing to be properly interpreted in relation to the observed flow patterns around the wing. This is believed to be the first time that flow-induced pressures have been measured on a model in a flow-visualization water tunnel at such a low flow velocity.

## **RELEASE LIMITATION**

*Approved for public release*

DEPARTMENT OF DEFENCE  
DEFENCE SCIENCE & TECHNOLOGY ORGANISATION

**DSTO**

AQ F01-07-1423

*Published by*

*DSTO*

*Aeronautical and Maritime Research Laboratory*

*PO Box 4331*

*Melbourne Victoria 3001*

*Telephone: (03) 9626 7000*

*Fax: (03) 9626 7999*

*© Commonwealth of Australia 2000*

*AR-011-650*

*November 2000*

**APPROVED FOR PUBLIC RELEASE**

# An Investigation into the Feasibility of Measuring Flow-Induced Pressures on the Surface of a Model in the AMRL Water Tunnel

## Executive Summary

A study has been undertaken to assess the feasibility of measuring flow-induced pressures on the surface of a model in the AMRL flow-visualization water tunnel. These pressures are extremely small due to the low free-stream velocities generally used for flow-visualization experiments in the tunnel. For a free-stream velocity of 0.1 m/s, which corresponds to a dynamic pressure of about 5 Pa, flow-induced pressures are typically less than about 15 Pa. In the past these pressures could not be measured accurately due to the unavailability of suitable pressure transducers. In this report it is shown that it is now possible to measure the pressures using a modern highly-sensitive differential pressure transducer, having a total range of 20 Pa.

A wide range of flow-induced pressures was measured on a delta wing in the AMRL water tunnel, and at the same time the vortical flow over the wing was visualized using sodium fluorescein dye. The wing was fitted with pressure tapings arranged in spanwise rows. Pressures were measured for angles of incidence of 24°, 27° and 30°, for an angle of sideslip of 0°. The nominal free-stream velocity used in the experiments was 0.1 m/s, giving a Reynolds number of about  $3.0 \times 10^4$  (based on the wing centreline chord of 300.0 mm).

Pressure coefficients measured on the wing in the water tunnel were found to be in good agreement with corresponding published wind-tunnel data, for the limited comparisons made, thus giving credibility to the current work. This is believed to be the first time that flow-induced pressures have been measured on a model in a flow-visualization water tunnel at such a low flow velocity. Simultaneous pressure measurement and visualization of the flow will enable measured pressure distributions to be properly interpreted in terms of the observed flow patterns. In the past it has generally been necessary to carry out complementary wind-tunnel experiments, using a larger model and a higher free-stream velocity, to obtain the required pressure loading. The new capability will be useful for a number of applications, including the validation of computational-fluid-dynamic (CFD) codes, the assessment of the effects of aircraft modifications on aircraft loading, and basic aerodynamics research.

## Author



### **Lincoln P. Erm**

**Air Operations Division**

*Lincoln Erm obtained a Bachelor of Engineering (Mechanical) degree in 1967 and a Master of Engineering Science degree in 1969, both from the University of Melbourne. His Master's degree was concerned with the yielding of aluminium alloy when subjected to both tensile and torsional loading. He joined the Aeronautical Research Laboratories (now called the Aeronautical and Maritime Research Laboratory) in 1970 and has worked on a wide range of research projects, including the prediction of the performance of gas turbine engines under conditions of pulsating flow, parametric studies of ramrocket performance, flow instability in aircraft intakes and problems associated with the landing of a helicopter on the flight deck of a ship. Concurrently with some of the above work, he studied at the University of Melbourne and in 1988 obtained his Doctor of Philosophy degree for work on low-Reynolds-number turbulent boundary layers. Lincoln is currently employed as a Research Scientist and is undertaking research investigations in the low-speed wind tunnel and the water tunnel.*

---

## Contents

1. INTRODUCTION .....	1
2. GENERAL DISCUSSION ON THE MEASUREMENT OF FLOW- INDUCED PRESSURES .....	2
2.1 Use of Pressure Tappings.....	2
2.2 Difficulties Associated with Measuring Pressures.....	2
3. MEASUREMENT OF FLOW-INDUCED PRESSURES ON A DELTA WING.....	3
3.1 Description of AMRL Water Tunnel.....	3
3.2 Details of Delta Wing .....	5
3.3 Instrumentation Used to Measure Pressures .....	7
3.4 Experimental Setup .....	8
3.5 Scope of Experiments and Experimental Procedure .....	10
3.6 Analysis of Experimental Results .....	11
4. CONCLUDING REMARKS .....	20
5. ACKNOWLEDGEMENTS .....	20
6. REFERENCES .....	21

## Notation

$c$	Centreline chord of the delta wing ( $c = 300.0$ mm).
$C_p$	Pressure coefficient on the surface of the delta wing.
$p_{\text{ref}}$	Static pressure measured by the reference static-pressure probe, (Pa).
$P_{\text{ref}}$	Total pressure measured by the reference total-pressure probe, (Pa).
$p_{\text{wing}}$	Flow-induced pressure at a pressure tapping on the delta wing, (Pa).
$R$	Reynolds number for the delta wing in water, ( $R = Uc/\nu_w$ ).
$s$	Local semi-span of the delta wing, (mm).
$U$	Free-stream velocity in the test section of the water tunnel, (m/s).
$x$	Chordwise distance from the apex of the delta wing, (mm).
$y$	Spanwise distance from the centreline chord of the delta wing, (mm).
$\alpha$	Angle of incidence of the delta wing, (degrees).
$\beta$	Angle of sideslip of the delta wing, (degrees).
$\nu_w$	Kinematic viscosity of water, ( $\text{m}^2/\text{s}$ ).
$\rho_a$	Density of air, ( $\text{kg}/\text{m}^3$ ).
$\rho_w$	Density of water, ( $\text{kg}/\text{m}^3$ ).

## 1. Introduction

Water tunnels are ideal for carrying out flow-visualization studies using models of vehicles such as modern high-performance aircraft. Different techniques can be used to visualize the flow patterns, including using dyes emitted from ports strategically located on the model, using hydrogen bubbles generated at selected regions on the model, and by illuminating fluorescent dyes in the flow using lasers. Flow-visualization studies can give an insight into the complex vortical flow behaviour around models, enabling researchers to obtain an understanding of the basic fluid dynamics of the flows. Flow-visualization is a useful tool when undertaking developmental work in water tunnels. Such testing in water tunnels is appealing since models are relatively cheap to build and modify (compared with wind-tunnel models), so that experiments can be undertaken and results evaluated quickly.

Despite the usefulness of water tunnels in helping researchers understand flow behaviour, experimental investigations in water tunnels do have their limitations. The optimum free-stream velocity to use for flow-visualization experiments is low, being typically about 0.1 m/s, which corresponds to a dynamic pressure of about 5 Pa. A low velocity is needed to preserve the clarity of the flow structure. For such a low velocity, flow-induced changes in forces, moments and static pressures on a model are also low and such quantities are therefore difficult to measure accurately. If the data could be measured accurately in a water tunnel, it would be possible to determine the loading on a model in the tunnel while simultaneously viewing the flow pattern around the model. The calculated loading on the model could then be properly interpreted in relation to the observed flow patterns around the model. In the past it has generally been necessary to carry out complementary wind-tunnel experiments, using a larger model and a higher free-stream velocity, to obtain accurate force, moment and pressure data corresponding to an observed flow pattern. Such data can be measured without difficulty in a wind tunnel since the quantities are generally large, but there can be problems in correlating the wind-tunnel quantitative data with the water-tunnel flow-visualization results, due to the different experimental conditions.

The problem of measuring the small flow-induced forces and moments on models in flow-visualization water tunnels has recently been addressed by Suárez, Ayers & Malcolm (1994), who developed a multi-component strain-gauge balance to measure the forces and moments. The balance was designed to measure normal and side forces (but not an axial force), as well as yawing, pitching and rolling moments. The balance was mounted inside a water-tunnel model and was used in a manner similar to wind-tunnel balances. Forces and moments were measured on a model of an aircraft in a water tunnel and compared with corresponding measurements taken in a wind tunnel. The water-tunnel loads were small (typical normal force was about 0.9 N), but good agreement was obtained between the two sets of data, indicating that water tunnels can be used effectively for quantitative as well as qualitative measurements. Associated



work on force/moment balances has been reported by Suárez & Malcolm (1994), Suárez et al. (1994) and Suárez & Malcolm (1995).

The above work on the measurement of small flow-induced forces and moments in a flow-visualization water tunnel significantly increases the usefulness of such facilities, but there did not seem to be any associated published work on the measurement of small flow-induced pressures on the surface of a model in such a tunnel. This report gives details of an experimental investigation undertaken to assess whether it is feasible to measure such pressures. The study was carried out in the flow-visualization water tunnel at the Aeronautical and Maritime Research Laboratory (AMRL) using a model of a delta wing. It is shown that it is possible to measure the pressures using a modern low-range pressure transducer, provided special precautions are taken. Flow-induced pressures were measured on the delta wing for three different angles of incidence and at the same time the leading-edge vortical flow over the wing was visualized for each case.

## **2. General Discussion on the Measurement of Flow-Induced Pressures**

### **2.1 Use of Pressure Tappings**

To measure the flow-induced pressure at a given location on the surface of a model in a flow-visualization water tunnel it is first necessary to fit a pressure tapping at that location. A tapping is formed by inserting a metal tube of small diameter (external diameter is typically 1.5 mm) through the surface of the model at the required location so that the longitudinal axis of the tube is normal to the surface and the orifice of the tube is flush with the surface. A flexible plastic tube is usually used to connect the metal tube to one of the ports of a differential pressure transducer, and likewise a reference probe located in the tunnel is connected to the other port on the transducer, thereby enabling the flow-induced pressure to be measured.

### **2.2 Difficulties Associated with Measuring Pressures**

The measurement of flow-induced pressures on a model in a flow-visualization water tunnel is a more difficult task than the measurement of corresponding pressures in a wind tunnel. For such a water tunnel, the flow-induced pressures are generally far smaller than for a wind tunnel due to the low water velocities used. For a water tunnel operating at a free-stream velocity,  $U$ , of 0.1 m/s, a typical velocity used in flow-visualization experiments, the free-stream dynamic pressure, i.e.  $0.5\rho_w U^2$ , is about 5 Pa, where  $\rho_w$  is the density of water. Such low pressures can only be measured

accurately using the most sensitive pressure transducers currently available. By contrast, for a wind tunnel operating at a free-stream velocity of 60 m/s, the free-stream dynamic pressure, i.e.  $0.5\rho_a U^2$ , is about 2150 Pa, where  $\rho_a$  is the density of air.

A differential pressure transducer suitable for measuring flow-induced pressures in a flow-visualization water tunnel has a full-scale range of  $\pm 0.1$  mbar =  $\pm 10$  Pa, i.e. about  $\pm 1.0$  mm of water (see Section 3.3 for details of the transducer used at AMRL). A difficulty associated with measuring flow-induced pressures in such a water tunnel is that pressures caused by heads of water are critically important and it is essential that all tubes connecting pressure tapings and reference probes to the transducer are completely filled with water at all times. Small air bubbles in the tubes can cause errors in measured pressures that are large relative to the flow-induced pressures on a model. An air bubble of height 0.1 mm in the tubes can cause measured flow-induced pressures to be in error by about 10% of the full-scale reading of the transducer. This problem does not arise when measuring pressures in a wind tunnel since the working fluid, i.e. air, is the same in the tubes, the tunnel and the atmosphere, without any fluid interfaces.

To minimise any possible errors in the measurements caused by local variations in the water level near the model when water flows over the model, the tunnel velocity should be kept as low as possible, consistent with obtaining acceptable flow-visualization images. The model should also be located well below the water surface so that the deviation of the flow around the model, caused by the blockage of the model, has a negligible effect on the water level. There should not be any parts of the apparatus protruding through the water surface near the model since this could create ripples on the water surface which could affect the accuracy of the measurements. The sting attached to the model and the tubes connected to the pressure tapings and the reference probes should protrude through the water surface well downstream of the model.

### 3. Measurement of Flow-Induced Pressures on a Delta Wing

#### 3.1 Description of AMRL Water Tunnel

The experimental investigation was carried out in an Eidetics<sup>1</sup> Model 1520 flow-visualization water tunnel, shown diagrammatically in Figure 1. The facility has a horizontal-flow test section 1520 mm long, 510 mm deep and 380 mm wide and the tunnel is constructed so that it is possible to look directly upstream into the test section from a window at the downstream end of the diffuser. The free-stream velocity can be

---

<sup>1</sup> Eidetics Corporation, 3425 Lomita Boulevard, Torrance, CA, 90505, USA.

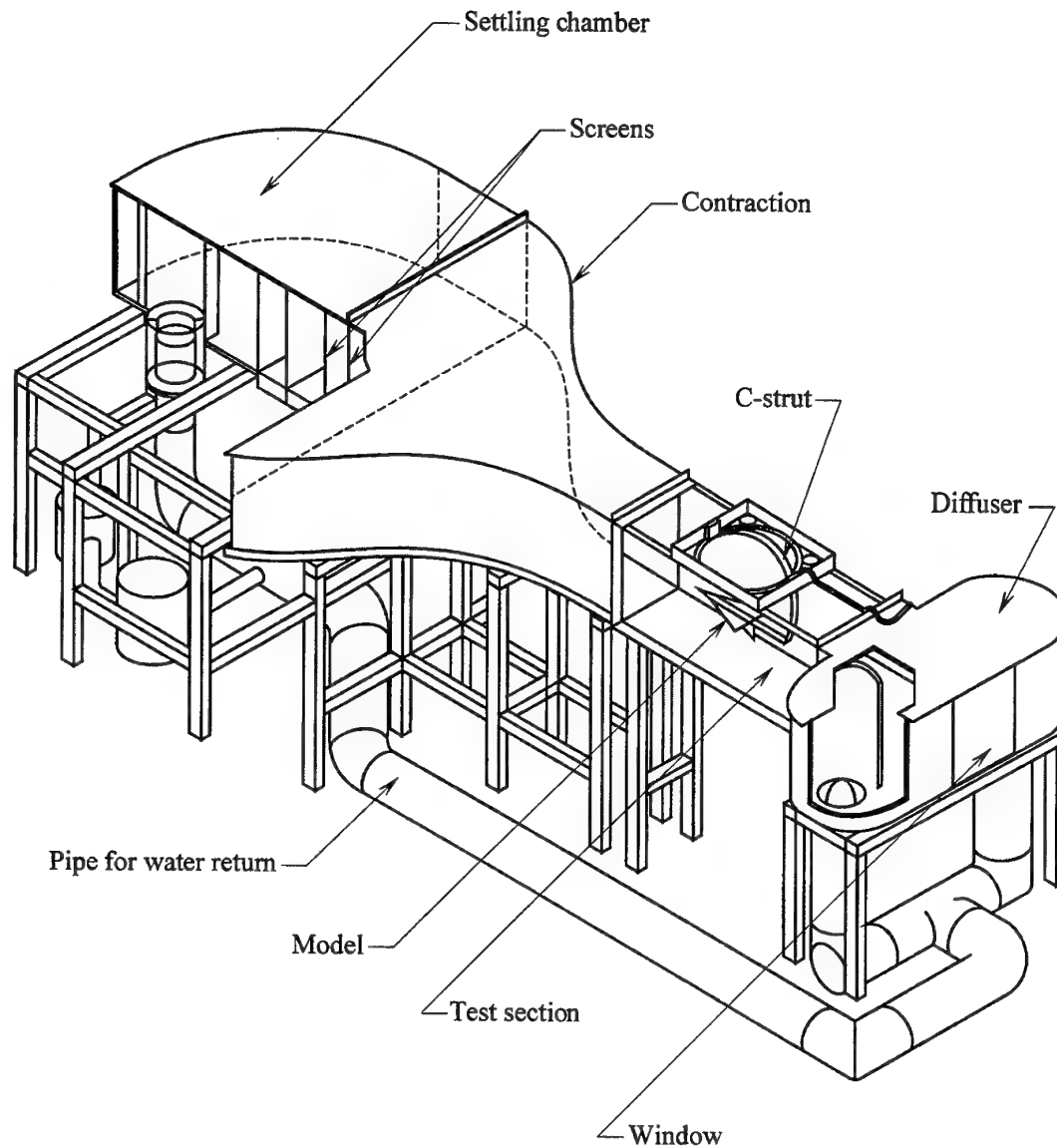


*Figure 1. Diagrammatic Representation of the Eidetics Model 1520  
Flow-Visualization Water Tunnel.*

varied between 0 and 0.6 m/s. There are six dye canisters on the tunnel that can be pressurised with air to force dye through plastic tubes to selected locations on a model for flow-visualization studies. The flow rate of dye in each circuit can be controlled independently using adjustable valves. Models can be mounted on a sting attached to a C-strut, which can be rotated in the vertical and horizontal planes to set the model at different pitch and yaw angles.

### 3.2 Details of Delta Wing

A delta wing is an ideal test model for experiments involving simultaneous pressure measurement and flow visualization. The flow over a delta wing at an angle of incidence is dominated by two large bound vortices that are formed at the two leading-edges of the wing, due to flow separation at the leading edges, and these vortices produce intense suction peaks on the wing surface under the vortices. The relatively large values of the flow-induced pressures at the suction peaks facilitate the measurement of the pressures. Furthermore, numerous wind-tunnel investigations have been undertaken to measure flow-induced pressures on delta wings (for example, Fink & Taylor, 1967; Atashbaz & Ahmed, 1997), enabling the water-tunnel measurements to be compared with similar wind-tunnel data.

The delta wing used in the experiments is shown diagrammatically in Figure 2. The wing is made of clear Perspex<sup>TM</sup> and has a chord of 300.0 mm, a span of 218.4 mm and is 6.5 mm thick. The leading-edge sweep angle of the wing is 70°. The edges of the wing are square to the leeward<sup>2</sup> (suction) surface for the first 0.5 mm from that surface, and they are then bevelled at an angle of 30° to the leeward surface, as shown. The leeward surface of the wing contains 7 rows of pressure tapings, spaced at intervals of 30.0 mm (1/10th of the chord) from the trailing edge of the wing. The metal tube used for the tapings has an outer diameter of 1.6 mm and an inner diameter of 1.2 mm. For each of the rows, the tapings are symmetrically spaced at intervals of 1/20th or 1/40th of the local span at that row, as shown. Altogether there are 148 pressure tapings on the wing, with rows 1, 2, 3, 4, 5, 6 and 7 having 13, 15, 15, 25, 27, 27 and 26 tapings respectively. The central tapping is missing in row 7 since a sting (not shown in Figure 2) was attached to the wing at this tapping location. Rows 1 to 4 have fewer tapings than other rows due to spanwise spacing limitations for these rows and the fact that tapings were not inserted in the wing if they would have protruded into the bevelled portion of the wing. The metal tubes used for the tapings project about 3 mm out from the windward surface of the wing and then bend at 90° so that they are parallel to the wing chord and point in the general downstream direction. The total length of the bent projecting tubes is about 8 mm. These metal tubes were connected to the pressure transducer using flexible plastic tubes. The tubes on the windward side of the wing may have affected the flow slightly, but this was acceptable for the current study which was concerned with examining the feasibility of measuring flow-induced pressures.

A metal tube (not shown in Figure 2) was attached to the windward surface of the wing so that the outlet of the tube was close to the apex of the wing. The tube was connected to the dye system to enable the leading-edge vortices on the wing to be visualized using sodium fluorescein dye. The leeward surface of the wing was painted matt black to provide a contrasting background when obtaining flow-visualization images.

<sup>2</sup> Since the wing is mounted upside down in the tunnel, the terms windward and leeward are used instead of lower and upper respectively when referring to wing surfaces.

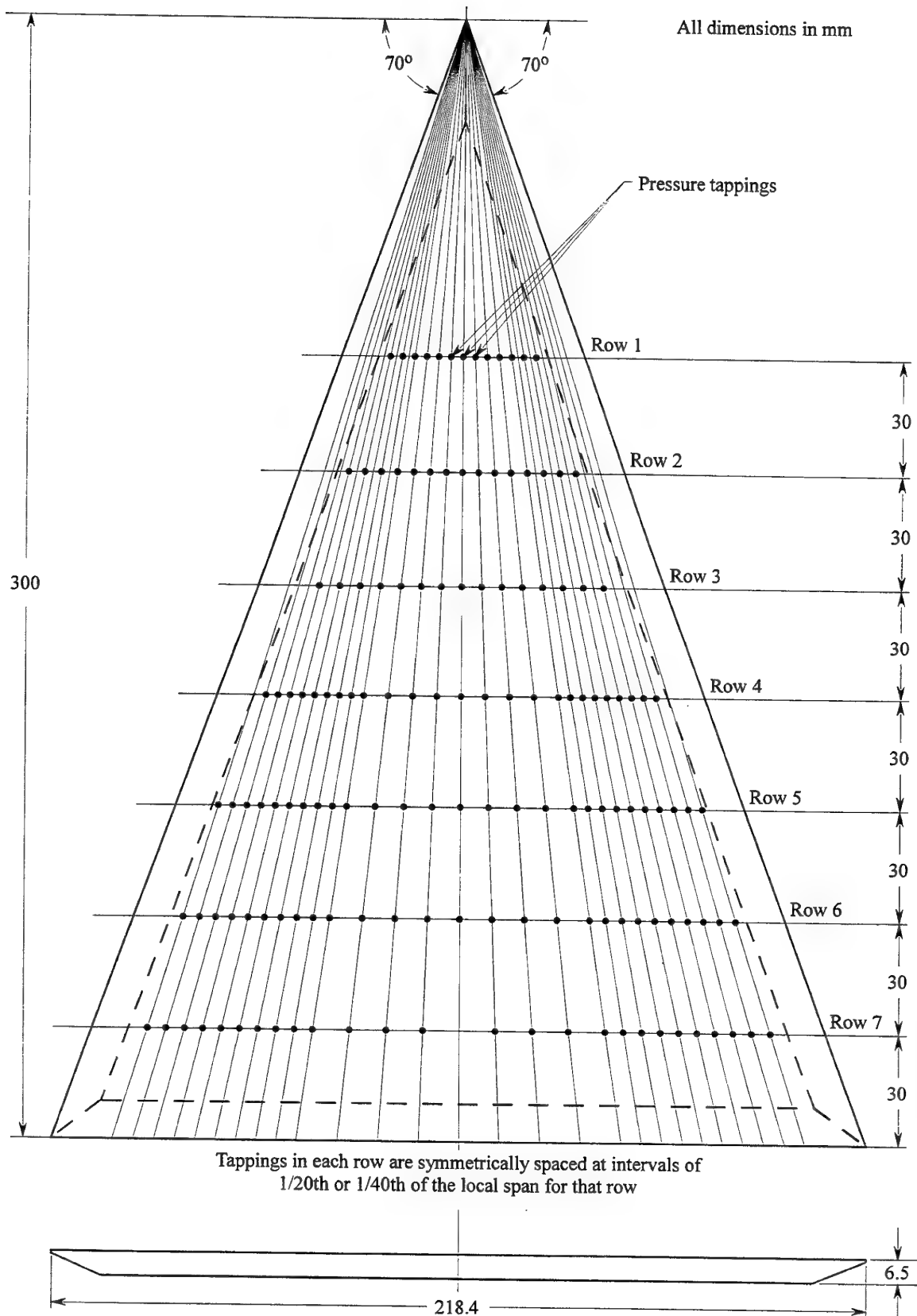


Figure 2. Diagrammatic representation of the delta wing, showing the locations of the pressure tappings.

### 3.3 Instrumentation Used to Measure Pressures

Flow-induced pressures were measured using a Druck<sup>3</sup> LPM 9481 Low Differential Pressure Sensor and a Druck DPI 282 Digital Pressure and Process Indicator.

The LPM 9481 Low Differential Pressure Sensor has a full-scale range of  $\pm 0.1$  mbar (i.e.  $\pm 10$  Pa). The pressure transducer operates on a supply voltage of 10 to 30 V d.c. and the output signal can vary within the range 0 to 5 V, with a signal of 2.5 V corresponding to zero differential pressure. The transducer has a response time of 10 ms and its diaphragm is made from beryllium copper.

To operate the pressure transducer it is convenient to interface it with the DPI 282 Digital Pressure and Process Indicator. The pressure indicator provides an excitation voltage of 24 V d.c.  $\pm 5\%$  for the transducer and the input signal range for the indicator can vary from  $-20$  to  $+20$  V. The transducer and the indicator were supplied as a calibrated matched pair and the indicator can display the transducer output voltage in terms of a pressure unit (such as Pa) selected by the operator. The combined non-linearity, hysteresis and repeatability performance specification of the Druck LPM 9481/DPI 282 pressure-measurement system is  $\pm 0.1\%$  maximum of the full-scale reading. An analog output voltage proportional to the displayed pressure reading can be provided by the pressure indicator. The analog voltage varies between 0 and 2 V and has an accuracy of  $\pm 0.05\%$  of the full-scale reading, so that the overall accuracy of the pressure-measurement system is  $\pm 0.15\%$ , i.e.  $\pm 0.1\% \pm 0.05\%$ .

The calibration of the pressure-measurement system was checked using the following procedure. A differential pressure was applied to the pressure transducer by connecting a water reservoir to each of the ports of the transducer. The level of the water in one of the reservoirs was fixed and the level in the other could be adjusted by moving the reservoir in the vertical direction using a sensitive traversing mechanism, thereby changing the differential pressure applied to the transducer. The level of the water in the adjustable reservoir was varied from 1.0 mm below the level in the fixed reservoir to 1.0 mm above the fixed level, in increments of 0.1 mm, corresponding to 21 applied differential pressures. This variation in water level corresponds to an approximate applied differential pressure range of  $-10$  Pa to  $+10$  Pa, which is the full-scale range of the transducer. The differential pressures indicated by the pressure-measurement system are plotted against the applied pressures in Figure 3. The 21 data points are represented by open circles. The straight line drawn on Figure 3 corresponds to the ideal case in which the indicated pressure readings are exactly the same as the applied pressures. The fact that the plotted data closely follow this line shows that the pressure-measurement system is extremely accurate and this gives credibility to subsequent measurements using the system.

<sup>3</sup> Druck Limited, Fir Tree Lane, Groby, Leicester, LE6 OFH, England, UK.

Australian Representative: M. B. & K. J. Davidson Pty Ltd, 1-3 Lakewood Bld, Braeside, Victoria, 3195.

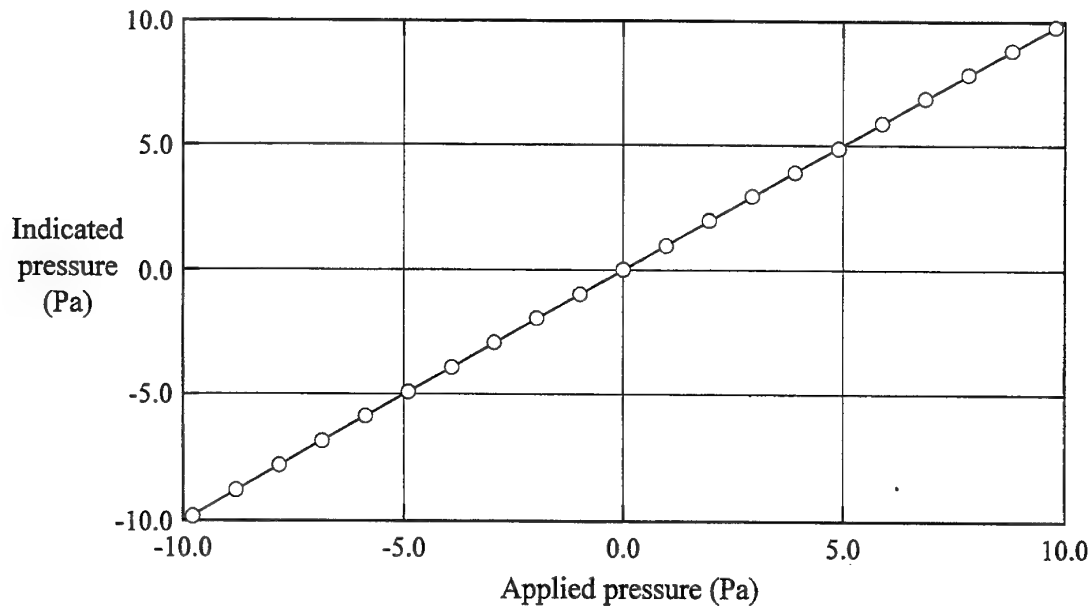
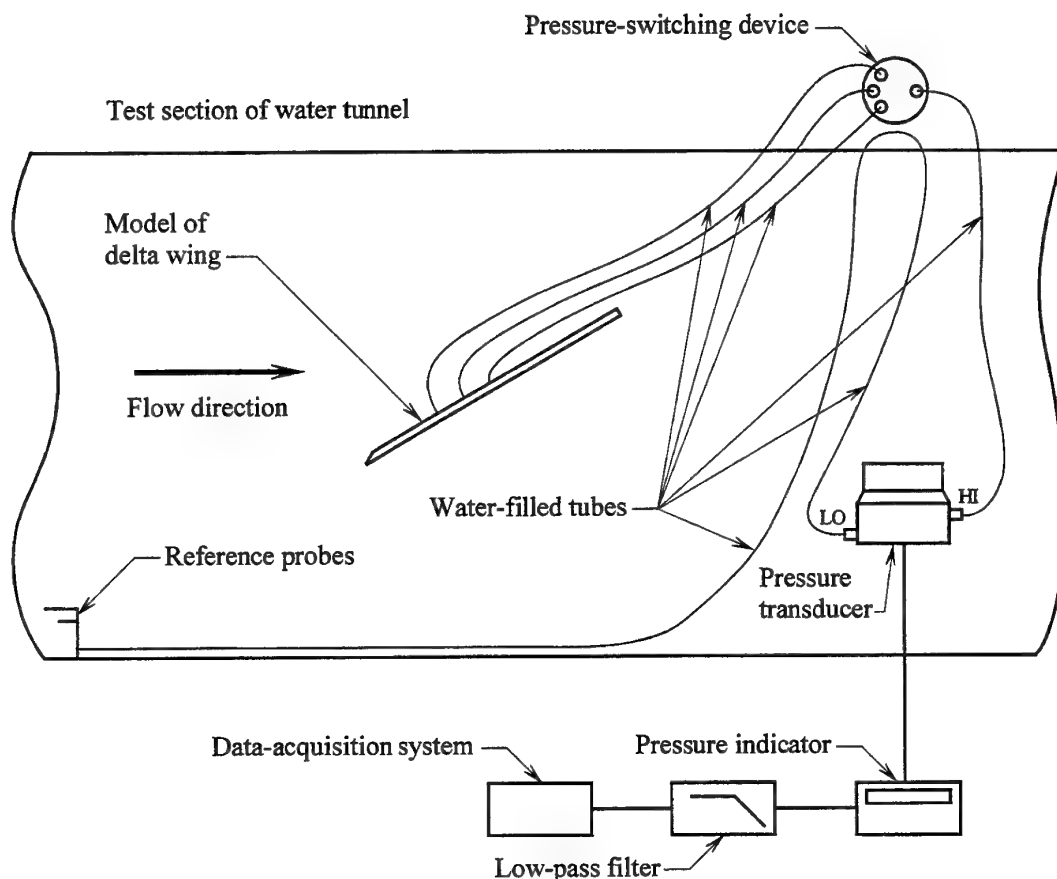


Figure 3. Indicated pressure vs applied pressure for the pressure-measurement system.  
 ○ experimental data; — ideal case.

### 3.4 Experimental Setup

Flow-induced pressures on the delta wing were measured using the experimental set up shown diagrammatically in Figure 4. The delta wing was attached to the C-strut on the tunnel (not shown in Figure 4), enabling the pitch and yaw angles of the wing to be varied. The pressure tapings on the wing were connected in turn to the HI port on the differential pressure transducer. A reference static-pressure probe and a reference total-pressure probe were positioned on the floor of the test section on the longitudinal centreline and they were located about 300 mm upstream of the apex of the wing. The reference pressure was measured using the static-pressure probe, which was connected directly to the LO port on the transducer. The reference pressure could have been measured at other locations in the tunnel, although it would not have been advisable to locate a reference probe in the flow-field close to the model. The output terminals of the Druck pressure-measurement system (see Section 3.3) were connected to the input terminals of a low-pass filter whose output terminals were connected in turn to an AMRL data-acquisition system.

It was important that the pressure transducer was oriented upright as shown, so that its pressure sensing element was horizontal, since otherwise there would have been a significant variation in hydrostatic pressure from the top to the bottom of the sensing element, which could have resulted in inaccurate pressure readings. The transducer can



*Figure 4. Diagrammatic representation of the experimental setup used to measure flow-induced pressures.*

withstand a differential overpressure of 500 mm of water before being damaged, so care was needed that excessive over-pressures were not applied inadvertently (such as by removing one of the tubes from the transducer and leaving a 500 mm head of water in the other tube).

Figure 4 shows that the different pressure tapings were connected to the pressure transducer via a pressure-switching device. In the current experiments, the tubes were in fact switched by hand, one at a time, to the transducer. A commercially-available pressure-switching device was initially tested, but it was found to be unsuitable since its water passages had a small cross-sectional area ( $\approx 0.25 \text{ mm}^2$ ) and they regularly became blocked with air bubbles or foreign particles in the water. A suitable pressure-switching device is currently being manufactured and will be used in future experiments.



### 3.5 Scope of Experiments and Experimental Procedure

Flow-induced pressures were measured on the delta wing for angles of incidence,  $\alpha$ , of  $24^\circ$ ,  $27^\circ$  and  $30^\circ$ , for an angle of sideslip,  $\beta$ , of  $0^\circ$ . The nominal free-stream velocity in the test section of the tunnel,  $U$ , was 0.1 m/s for all measurements, giving a Reynolds number,  $R = Uc/\nu_w$ , of about  $3.0 \times 10^4$ , where  $c = 300.0$  mm is the centreline chord of the delta wing and  $\nu_w$  is the kinematic viscosity of water. The boundary layers were laminar on both sides of the wing. Flow-induced pressures were measured at different values of  $y/s$  along rows 1, 2, 3, 4 and 6 on the wing, corresponding to values of  $x/c$  of 0.3, 0.4, 0.5, 0.6 and 0.8 respectively (see Figure 2), where  $y$  is the spanwise distance from the centreline chord of the wing,  $s$  is the local semi-span of the wing and  $x$  is the chordwise distance from the apex of the wing. Flow-visualization images of the leading-edge vortices were also obtained for each of the three angles of incidence.

In this report, flow-induced pressures on the delta wing are presented as pressure coefficients,  $C_p$ , defined as follows:

$$C_p = \frac{(p_{\text{wing}} - p_{\text{ref}})}{(P_{\text{ref}} - p_{\text{ref}})} \quad (1)$$

where  $p_{\text{wing}}$  is a flow-induced pressure on the delta wing,  $p_{\text{ref}}$  is a static pressure measured by the reference static-pressure probe and  $P_{\text{ref}}$  is a total pressure measured by the reference total-pressure probe.

Differential pressures appearing in equation 1 were measured by connecting the appropriate probes/tappings to the ports on the differential pressure transducer and sampling the fluctuating output voltages of the low-pass filters using an AMRL data-acquisition system (see Section 3.4 for details of the experimental setup). The filters were set at 30 Hz and each voltage was sampled 100 times at a sampling frequency of 1 Hz. The 100 individual samples were then averaged to obtain mean values of differential pressures, which were used when computing values of  $C_p$ .

Pressure coefficients on the delta wing were obtained one row at a time by measuring differential pressures in the following order:

- (1)  $(P_{\text{ref}} - p_{\text{ref}})$ , reference pressures, (1 mean value),
- (2)  $(p_{\text{wing}} - p_{\text{ref}})$ , flow-induced pressures on the delta wing, (13 to 27 mean values),
- (3)  $(P_{\text{ref}} - p_{\text{ref}})$ , reference pressures, (1 mean value).

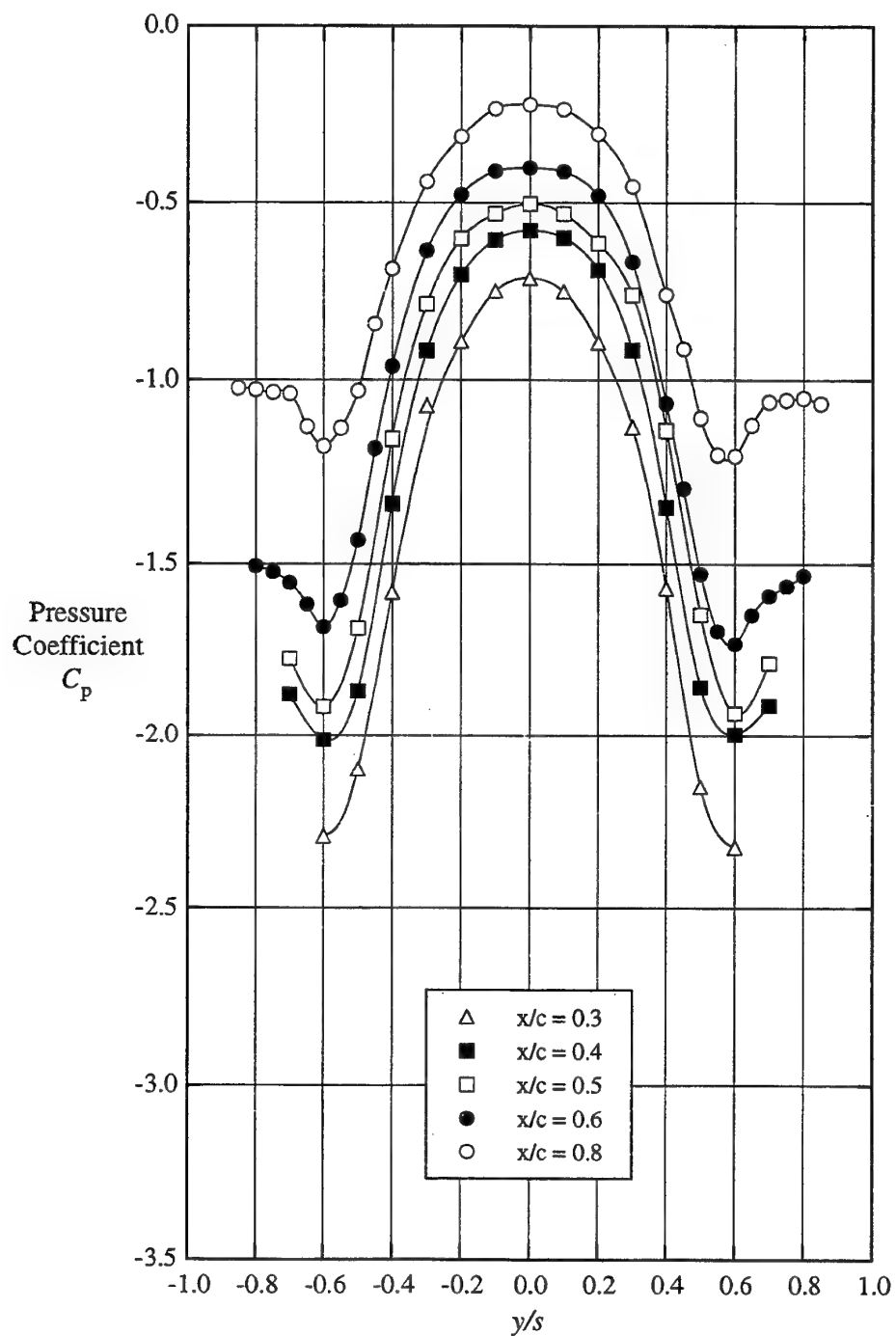
The reference pressures,  $(P_{\text{ref}} - p_{\text{ref}})$ , were measured both before and after the pressures on the wing,  $(p_{\text{wing}} - p_{\text{ref}})$ , to determine the changes in  $(P_{\text{ref}} - p_{\text{ref}})$  throughout an experimental run. The variation in  $(P_{\text{ref}} - p_{\text{ref}})$  was generally less than 2% for each set of measurements. Linear interpolation was used to determine the appropriate values of  $(P_{\text{ref}} - p_{\text{ref}})$  to use in equation 1 when computing values of  $C_p$  for the different pressureappings.

In these experiments, the method used to connect the probes/tappings to the differential pressure transducer was slightly more complicated than that normally used. A conventional method of connecting probes/tappings to a transducer is to connect a reference static-pressure probe to the LO port and to connect a reference total-pressure probe or pressure tapings to the HI port. With this arrangement, the free-stream dynamic pressure in the test section (reference total pressure – reference static pressure) is registered as a positive differential pressure and the flow-induced pressure on the delta wing (pressure at a tapping – reference static pressure) is registered as a negative differential pressure. The range of the differential pressure transducer used in the experiments was 20 Pa, i.e. –10 Pa to +10 Pa (see Section 3.3). Using the above connections, it was found that the magnitude of positive differential pressures plus the magnitude of negative differential pressures was often greater than 20 Pa. To overcome this difficulty, it was necessary in the experiments to reverse the connection of the reference static-pressure probe, depending on which differential pressures were being measured. When measuring free-stream dynamic pressures, the reference static-pressure probe was connected to the HI port on the transducer and the reference total-pressure probe was connected to the LO port. When measuring flow-induced pressures on the delta wing, the reference static-pressure probe was connected to the LO port and the pressure tapings on the wing were connected to the HI port. It was also necessary to adjust the zero setting on the transducer to incorporate a permanent offset in its reading, so that the transducer registered a finite differential pressure when in fact the applied differential pressure was zero. This ensured that the transducer output did not exceed the range –10 Pa to +10 Pa. Checks showed that the calibration of the pressure-measurement system was unaffected by the adjustment to the zero setting of the transducer.

The leading-edge vortices were visualized using sodium fluorescein dye injected from a single metal tube whose outlet was close to the apex of the delta wing. The dye from the tube divided into two streams, which passed into the cores of the leading-edge vortices on both sides of the wing, enabling the two vortices to be visualized simultaneously. Lighting was provided using incandescent globes strategically located around the test section. The images were captured using a Nikon™ Coolpix 950 digital camera, located alternatively at the side of the test section and directly underneath the test section. These images are matched with corresponding pressure measurements when discussing flow behaviour.

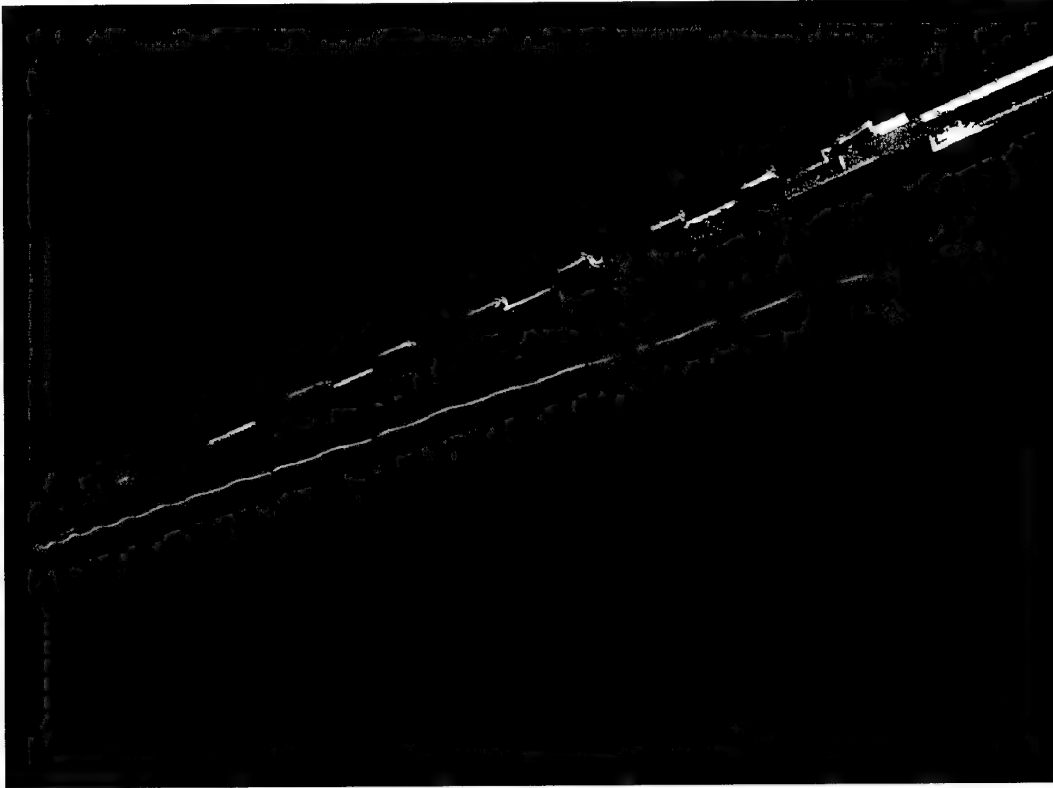
### 3.6 Analysis of Experimental Results

Measured pressure coefficients on the delta wing and corresponding side- and plan-view images of the leading-edge vortices are shown in Figures 5, 6 and 7 for angles of incidence of 24°, 27° and 30° respectively. Pressure coefficients are given for five spanwise rows of pressure tapings, corresponding to values of  $x/c$  of 0.3, 0.4, 0.5, 0.6 and 0.8. Each figure enables the  $C_p$  distributions to be correlated directly with the images of the vortical flow, which apply to the same flow conditions.

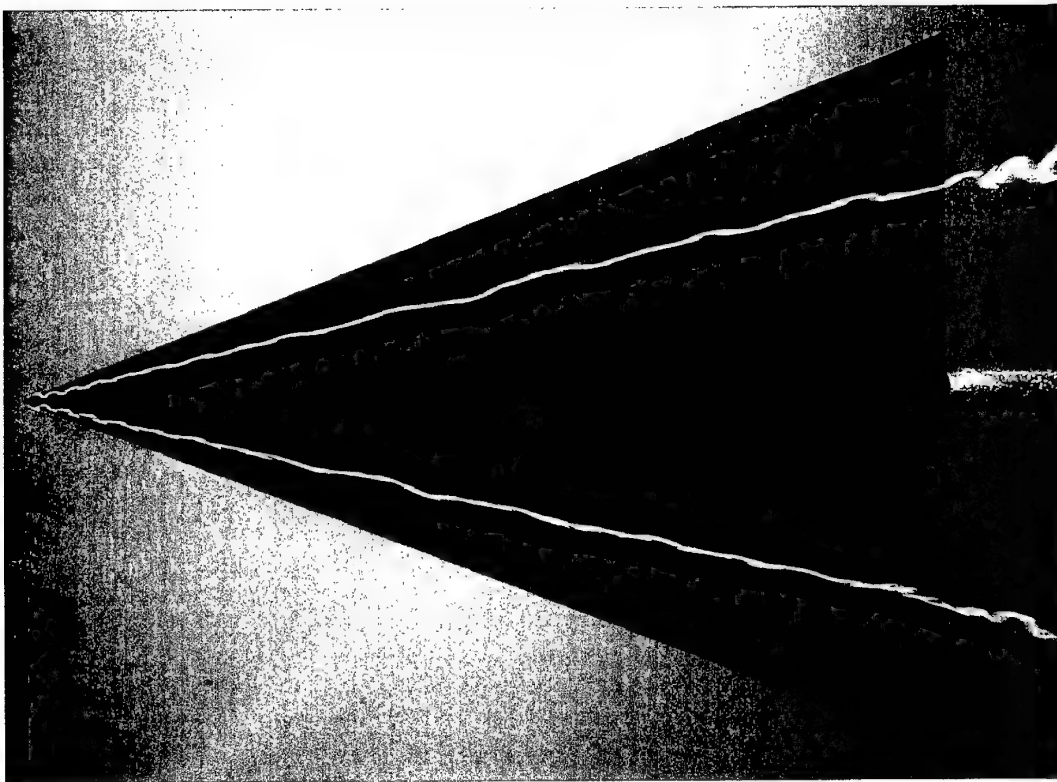


(a) pressure coefficients

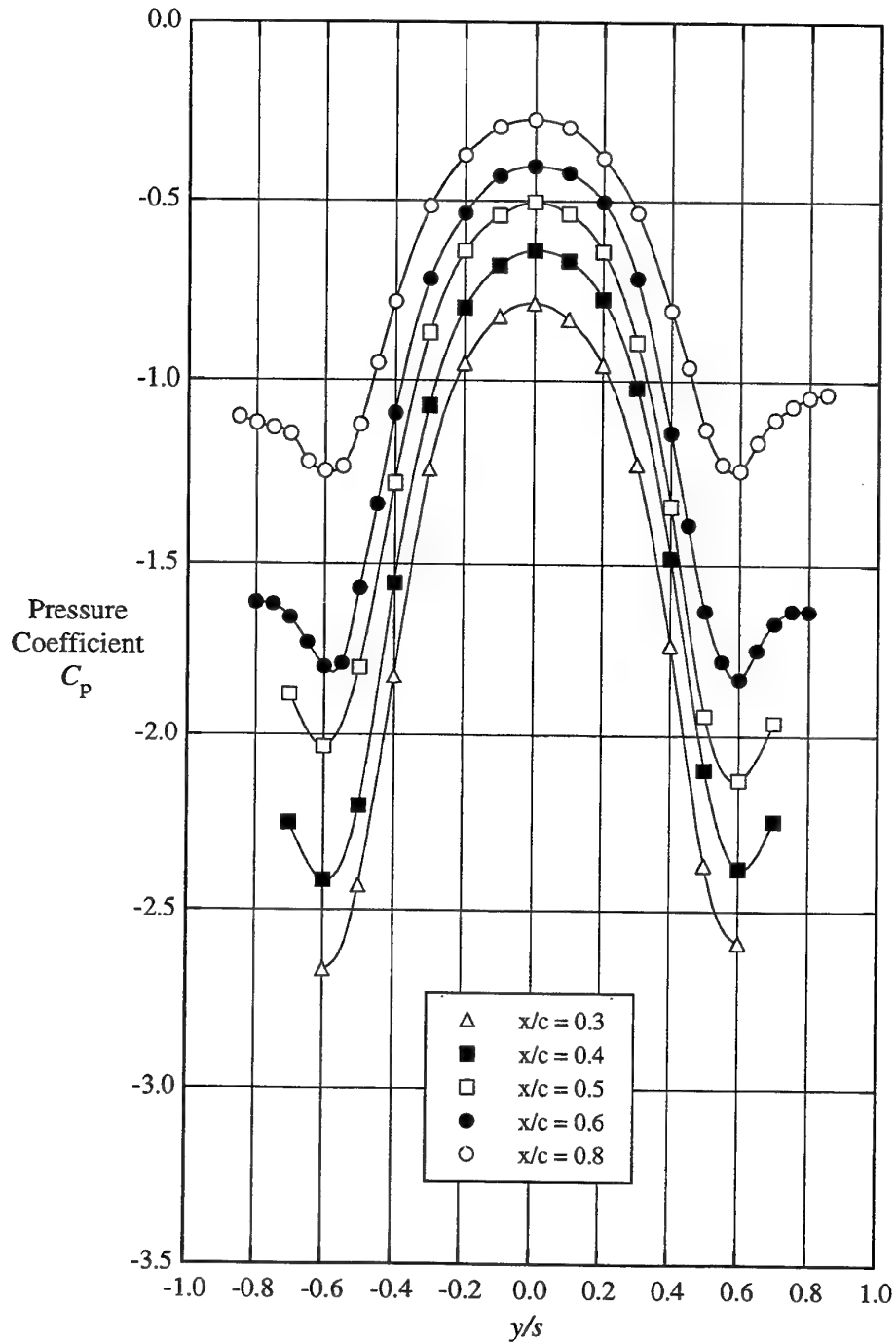
Figure 5. Characteristics of the flow over a delta wing for  $\alpha = 24^\circ$ .



*(b) side-view image of the vortical flow*

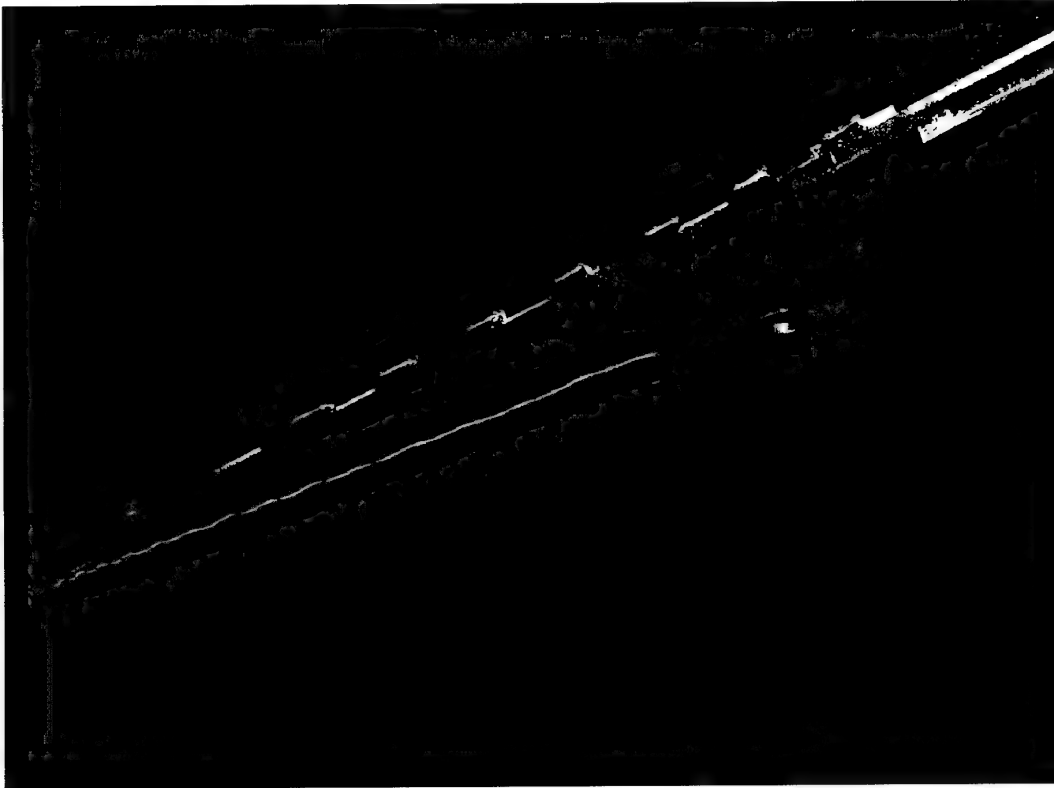


*(c) plan-view image of the vortical flow*

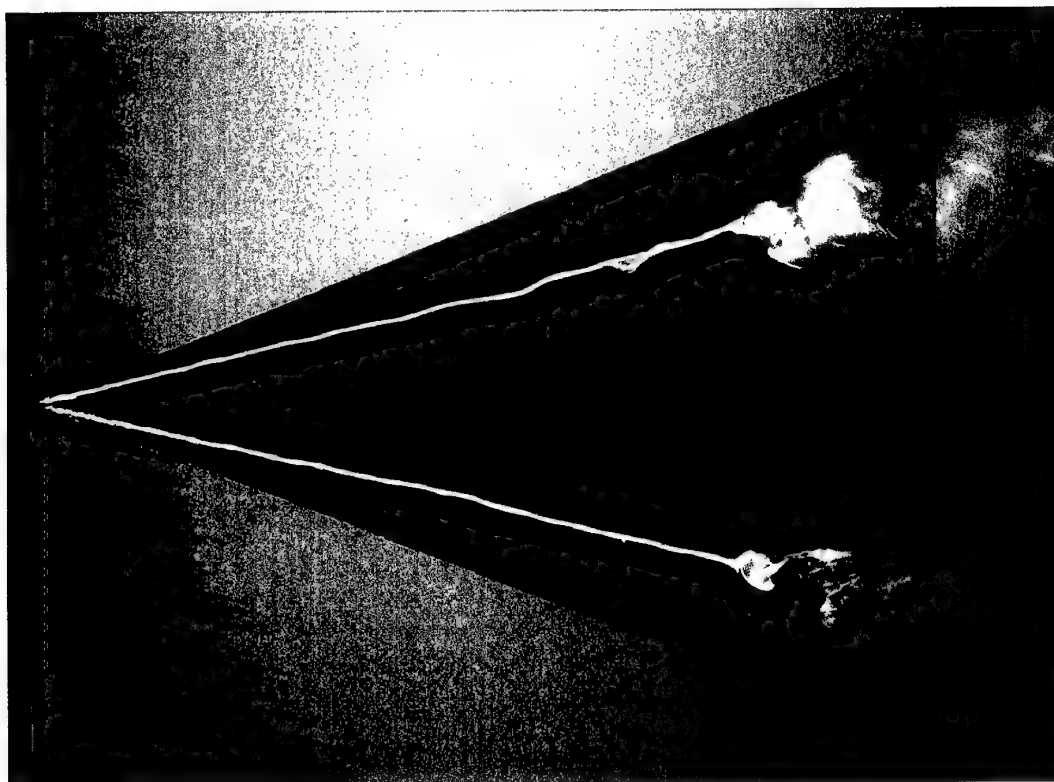


(a) pressure coefficients

Figure 6. Characteristics of the flow over a delta wing for  $\alpha = 27^\circ$ .

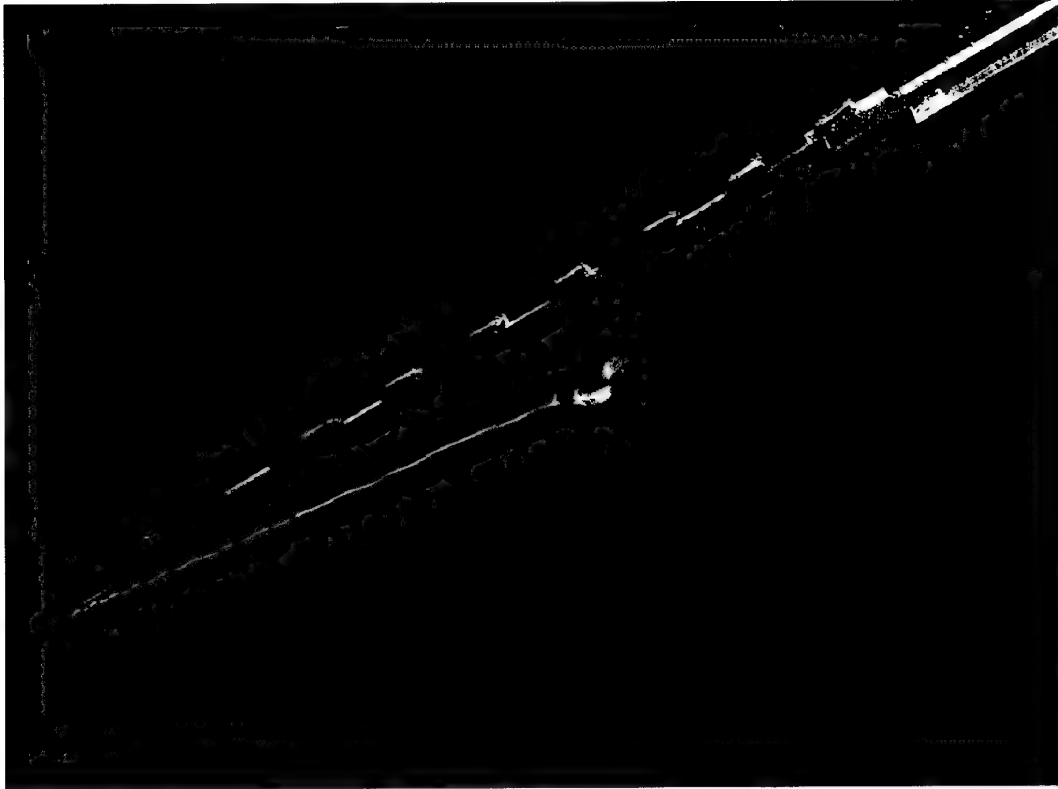


*(b) side-view image of the vortical flow*

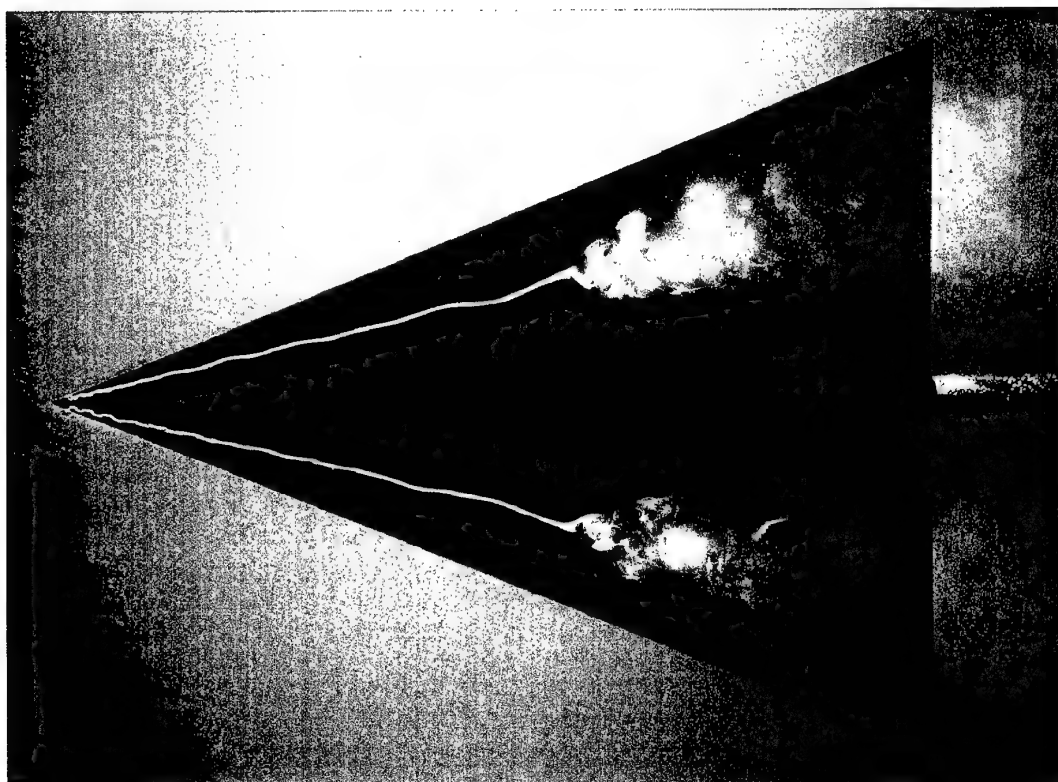


*(c) plan-view image of the vortical flow*

*Figure 6 cont'd. Characteristics of the flow over a delta wing for  $\alpha = 27^\circ$ .*



*(b) side-view image of the vortical flow*



*(c) plan-view image of the vortical flow*

*Figure 7 cont'd. Characteristics of the flow over a delta wing for  $\alpha = 30^\circ$ .*

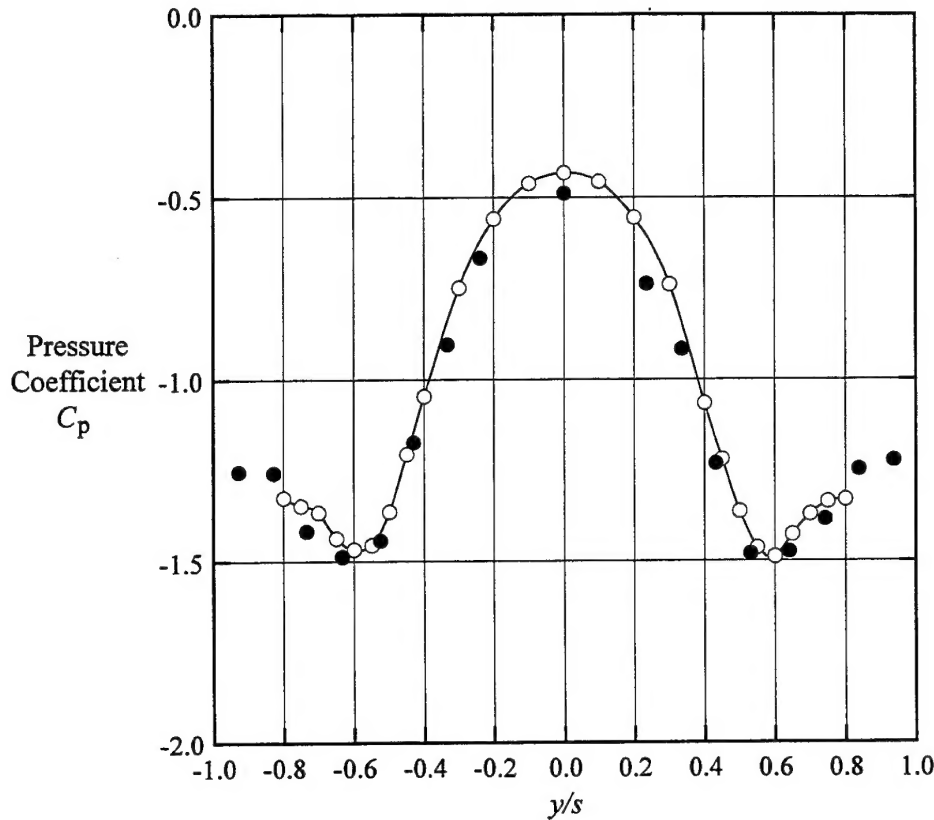


Figure 8. Comparison between pressure coefficients measured on a delta wing in the AMRL water tunnel and in a wind tunnel for  $\alpha = 30^\circ$  and  $x/c = 0.75$ .

○ Water-tunnel data; ● wind-tunnel data (Atashbaz & Ahmed, 1997).

respectively. This suggests that the technique of measuring flow-induced pressures in a low-velocity flow-visualization water tunnel has merit and is viable.

As indicated in Section 3.3, the accuracy of the pressure-measurement system is  $\pm 0.15\%$  of its full-scale readout. The system has an output voltage range of 0 to 2 V, corresponding to a pressure range of  $\pm 10$  Pa, so measured differential pressures are therefore accurate to within  $\pm 0.015$  Pa. The accuracy to which values of  $C_p$  can be measured is variable and depends on the actual system output voltages associated with each measurement. For flow-induced pressures corresponding to the mid range of the system, measured values of  $C_p$  are accurate to within about  $\pm 0.5\%$ .



## 6. References

- Atashbaz, G. & Ahmed, N. A. 1997, 'Asymmetry of vortex flow over slender delta wings'. *International Aerospace Congress 97*, Sydney, Australia, 24-27 February, pp. 41-52.
- Fink, P. T. & Taylor, J. 1967, 'Some early experiments on vortex separation'. 'Part II. -Some low speed experiments with 20 deg. delta wings.' *Aeronautical Research Council, R&M 3489*.
- Hummel, D. 1978, 'On the vortex formation over a slender wing at large angles of incidence'. *Agard Conference Proceedings 247*, High Angle of Attack Aerodynamics, Sandefjord, Norway, 4-6 October.
- Lambourne, N. C. & Bryer, D. W. 1962, 'The bursting of leading-edge vortices -some observations and discussion of the phenomenon'. *Aeronautical Research Council, R&M 3282*.
- Suárez, C. J., Ayers, B. F. & Malcolm, G. N. 1994, 'Force and moment measurements in a flow visualization water tunnel'. *AIAA 94-0673*, presented at the 32nd Aerospace Sciences Meeting & Exhibit, Reno, NV, USA, 10-13 January, pp. 1-12.
- Suárez, C. J. & Malcolm, G. N. 1994, 'Water tunnel force and moment measurements on an F/A-18'. *AIAA 94-1802-CP*, presented at the AIAA Applied Aerodynamics Conference, Colorado Springs, CO, USA, 20-22 June, pp. 12-24.
- Suárez, C. J., Malcolm, G. N., Kramer, B. R., Smith, B. C. & Ayers, B. F. 1994, 'Development of a multicomponent force and moment balance for water tunnel applications, Volumes I and II'. *NASA Contractor Report 4642*.
- Suárez, C. J. & Malcolm, G. N. 1995, 'Dynamic water tunnel tests for flow visualization and force/moment measurements on maneuvering aircraft'. *AIAA 95-1843-CP*, presented at the 13th AIAA Applied Aerodynamics Conference, San Diego, CA, USA, 19-22 June, pp. 658-670.

## **DISTRIBUTION LIST**

An Investigation into the Feasibility of Measuring Flow-Induced Pressures  
on the Surface of a Model in the AMRL Water Tunnel

Lincoln P. Erm

### **AUSTRALIA**

#### **DEFENCE ORGANISATION**

##### **Task Sponsor**

##### **S&T Program**

Chief Defence Scientist	} shared copy
FAS Science Policy	
AS Science Corporate Management	
Director General Science Policy Development	
Counsellor Defence Science, London (Doc Data Sheet only)	
Counsellor Defence Science, Washington (Doc Data Sheet only)	
Scientific Adviser to MRDC Thailand (Doc Data Sheet only)	
Scientific Adviser Policy and Command	
Navy Scientific Adviser (Doc Data Sheet and Distribution List only)	
Scientific Adviser - Army (Doc Data Sheet and Distribution List only)	
Air Force Scientific Adviser	
Director Trials	

##### **Aeronautical and Maritime Research Laboratory**

Director, W. H. Schofield	
Chief of Air Operations Division, C. R. Guy	
Research Leader Avionics and Flight Mechanics, N. Pollock	
Head Aerodynamic Applications, D. H. Thompson	
Head Flight Mechanics, N. Matheson	
Author, L. P. Erm (5 copies)	
G. D. Ainger	D. M. Carnell
J. C. Clayton	C. D. Edwards
M. Giacobello	M. K. Glaister
A. A. Gonzalez	G. R. Johnston
S. S. Lam	P. T. Malone
H. A. Quick	

**OTHER ORGANISATIONS**

NASA (Canberra)  
AusInfo

**OUTSIDE AUSTRALIA****ABSTRACTING AND INFORMATION ORGANISATIONS**

Library, Chemical Abstracts Reference Service  
Engineering Societies Library, US  
Materials Information, Cambridge Scientific Abstracts, US  
Documents Librarian, The Center for Research Libraries, US

**INFORMATION EXCHANGE AGREEMENT PARTNERS**

Acquisitions Unit, Science Reference and Information Service, UK  
Library - Exchange Desk, National Institute of Standards and Technology, US

**OTHER ORGANISATIONS**

Eidetics Corporation, 3425 Lomita Bld, Torrance, California, 90505, USA

SPARES (5 copies)

Total number of copies: 59